Report

Current Biology

# Recording electrical activity from the brain of behaving octopus

## Graphical abstract

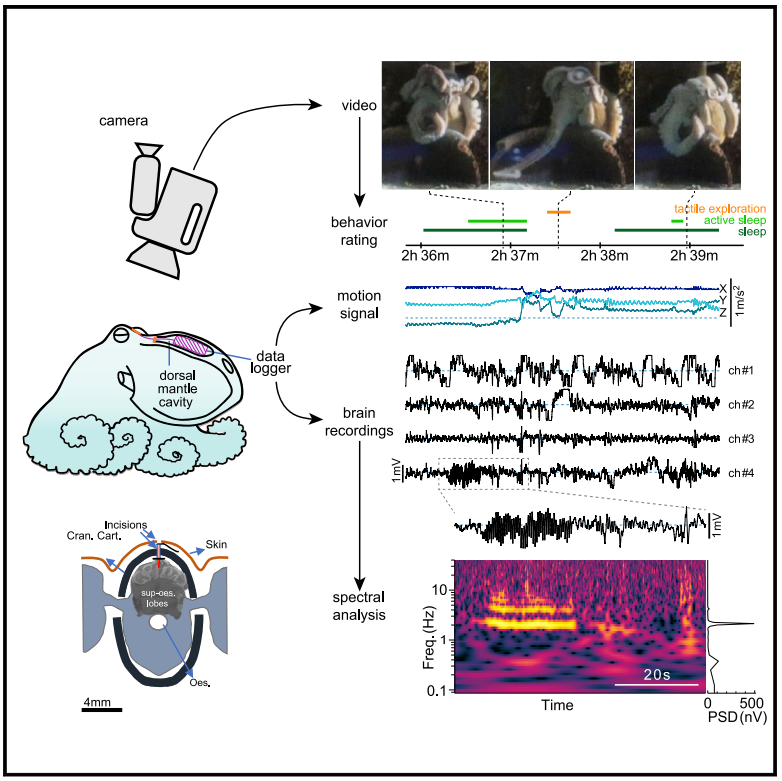


## Highlights

- First recordings of brain activity from untethered, freely moving octopus
- Electrodes implanted into learning and memory centers of the octopus brain
- Data logger surgically introduced into the animal's body
- 12 h of neural activity synchronized with HD video of untethered behavior

## Authors

Tamar Gutnick, Andreas Neef, Andrii Cherninskyi, Fabienne Ziadi-Künzli, Anna Di Cosmo, Hans-Peter Lipp, Michael J. Kuba

## Correspondence

tamar.gutnick@mail.huji.ac.il

## In brief

*In vivo* electrophysiology is an essential tool for correlating neural activity with animal behavior. This approach is very difficult in aquatic animals, and especially in the highly flexible, boneless octopus. Gutnick, Neef, Cherninskyi et al. now report the first recordings of brain activity from untethered, freely moving octopuses.

Gutnick et al., 2023, Current Biology *33*, 1171–1178
March 27, 2023 
https://doi.org/10.1016/j.cub.2023.02.006

CellPress

Current Biology

CellPress

Report

# Recording electrical activity from the brain of behaving octopus

Tamar Gutnick,[1,2,12,13,*] Andreas Neef,[3,4,5,6,7,8,12] Andrii Cherninskyi,[9,12] Fabienne Ziadi-Künzli,[10] Anna Di Cosmo,[2] Hans-Peter Lipp,[11] and Michael J. Kuba[1,2]

[1]Okinawa Institute of Science and Technology, Graduate University, Physics and Biology Unit, 904 0495 Okinawa, Japan
[2]Department of Biology, University of Naples Federico II, Via Cintia 26, 80126 Napoli, Italy
[3]Göttingen Campus Institute for Dynamics of Biological Networks, 37073 Göttingen, Germany
[4]Max Planck Institute for Dynamics and Self-Organization, 37077 Göttingen, Germany
[5]Bernstein Center for Computational Neuroscience, 37073 Göttingen, Germany
[6]Institute for the Dynamics of Complex Systems, University of Göttingen, 37075 Göttingen, Germany
[7]Max Planck Institute for Multidisciplinary Sciences, 37075 Göttingen, Germany
[8]Center for Biostructural Imaging of Neurodegeneration, 37075 Göttingen, Germany
[9]Bogomoletz Institute of Physiology, Kyiv 01024, Ukraine
[10]Okinawa Institute of Science and Technology, Graduate University, Nonlinear and Non-equilibrium Physics Unit, Okinawa 904-0495, Japan
[11]Institute of Evolutionary Medicine, Faculty of Medicine, University of Zurich, 8057 Zurich, Switzerland
[12]These authors contributed equally
[13]Lead contact
*Correspondence: tamar.gutnick@mail.huji.ac.il
https://doi.org/10.1016/j.cub.2023.02.006

## SUMMARY

Octopuses, which are among the most intelligent invertebrates,[1–4] have no skeleton and eight flexible arms whose sensory and motor activities are at once autonomous and coordinated by a complex central nervous system.[5–8] The octopus brain contains a very large number of neurons, organized into numerous distinct lobes, the functions of which have been proposed based largely on the results of lesioning experiments.[9–13] In other species, linking brain activity to behavior is done by implanting electrodes and directly correlating electrical activity with observed animal behavior. However, because the octopus lacks any hard structure to which recording equipment can be anchored, and because it uses its eight flexible arms to remove any foreign object attached to the outside of its body, *in vivo* recording of electrical activity from untethered, behaving octopuses has thus far not been possible. Here, we describe a novel technique for inserting a portable data logger into the octopus and implanting electrodes into the vertical lobe system, such that brain activity can be recorded for up to 12 h from unanesthetized, untethered octopuses and can be synchronized with simultaneous video recordings of behavior. In the brain activity, we identified several distinct patterns that appeared consistently in all animals. While some resemble activity patterns in mammalian neural tissue, others, such as episodes of 2 Hz, large amplitude oscillations, have not been reported. By providing an experimental platform for recording brain activity in behaving octopuses, our study is a critical step toward understanding how the brain controls behavior in these remarkable animals.

## RESULTS

### Data logger preparation

*In vivo* electrophysiological recording, a standard in many animal models, has proven immensely difficult in aquatic animals in general,[14] and particularly in octopuses. A major obstacle preventing such recordings is that octopuses will use their eight powerful, flexible arms to remove equipment attached anywhere on the outside of their body (Figure 1A). As a result, although there has been one report[15] of tethered recording from unrestrained animals in which the implanted electrodes are connected via wires to external recording equipment, this approach has not proved practical.

We solved this problem by adapting a data logger, initially developed for recording EEG activity during large-scale navigation experiments in free-flying birds,[16] for use inside the octopus (NeuroLogger; Figure 1B). The logger records and stores simultaneous data from 4 input and 2 reference channels for electric signals (sampled at 512 Hz), 3 accelerometer channels (sampled at 102 Hz), and an infrared (IR) receiver channel. Importantly, the logger does not rely on radio-telemetry, which is unsuitable for transmission through salt water. Adapting the loggers for use with octopuses required sealing it in a watertight casing. Therefore, we replaced the standard zinc/air batteries with voltage compatible nickel-metal hydride (NiMH) rechargeable batteries (Power One; Figure 1B). While zinc/air batteries allow for up to 47 h of recording, NiMH batteries limit our recordings to approximately 12 continuous hours of signal.

As no recording equipment could be attached to the outside surface of the octopus, we decided to implant the logger unit

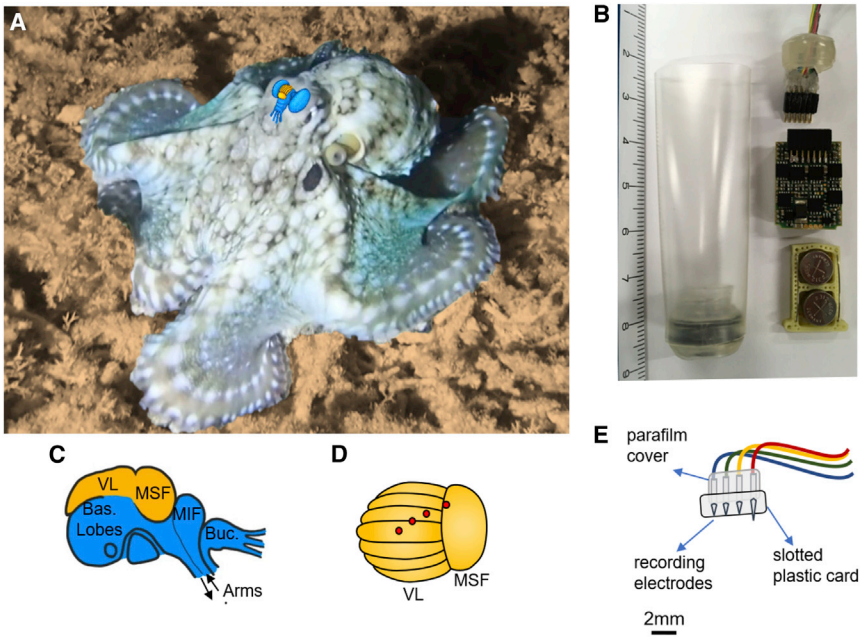


**Figure 1. Preparing data logger and electrodes for implanting into the MSF-VL in *Octopus cyanea***

(A) An *Octopus cyanea* in the wild with superimposed drawing of the central brain and optic lobes (blue) and medial superior frontal-vertical lobe (MSF-VL) complex (orange). (The background substrate in the image is color shifted so the octopus can be easily identified.) Image courtesy of Keishu Asada.

(B) Neurologger data loggers were powered by 2 nickel-metal hydride batteries (Power One ACCU Plus rechargeable p312). We created 2 plugs to seal the ends of the logger casing. Electrode wires were pre-threaded into one of the two plugs. The logger unit was sealed in a 25-mm heat shrink sleeve by gentle heating over the plugs. Dimension of the sealed logger was approximately 20 × 60 mm.

(C) Schematic of the supraoesophageal brain of the octopus. Our electrodes targeted the MSF-VL complex (in orange), the most dorsal area of the brain. Anatomical studies have shown that MSF inputs form *en passant* synapses with VL neurons.[9] The MSF-VL complex has been associated with visual learning. (VL, vertical lobe; MSF, median superior frontal lobe; MIF, median inferior frontal lobe; Buc. lobes, buccal lobes; Bas. lobes, basal lobes). See also Figure S1A.

(D) The size relationship between the 1-mm-spaced electrodes (red circles) and the MSF-VL complex. The electrode locations were reconstructed from microCT scans of the fixed, iodine-stained brain (see also Figures 2D, S1A, and S1B).

(E) The four recording electrodes were slotted through a precut plastic card. They were secured with cyanoacrylate glue and covered with Parafilm.

into the dorsal mantle cavity and to secure, under the skin, all wires connecting the logger to the electrodes. In benthic octopuses, the dorsal mantle cavities are elongated, isolated pockets, which run bilaterally within the dorsal muscle wall of the mantle, and are not connected with the shell rudiment or the ventral mantle cavity that contains the viscera (Figure 2A).[4] Taking into account the size of the logger (15 × 24 mm), we selected *Octopus cyanea* (*O. cyanea*), a large tropical octopus species, as our model animal (Figure 1A).[12] Adult *O. cyanea* weighs between 1.5 and 4 kg and have a mantle length of 20–35 cm. Available waterproof solutions for data loggers utilize rigid plastic housings, which are then attached outside the animal's body.[14] While rigid cases provide easier access to the logger, their size and shape is not suitable for implanting into even the largest animal. In constructing a waterproof casing, our main goal was to minimize the diameter of the final logger unit, thereby minimizing the necessary incision in the muscle wall. Therefore, using 25 mm heat shrink tubing, we created single-use, waterproof casings. The casing was sealed with end plugs, created by layering increasing diameters of heat shrink tubing. During preparation, copper electrode connector wires were pre-threaded through one of the end plugs (Figure 1B). The final sealed logger unit was 20 × 60 mm.

## Electrode implant

As a target for the recording, we selected the median superior frontal lobe (MSF)-vertical lobe (VL) complex of the octopus brain (Figures 1A, 1C, 1D, and S1A). Its location on the topmost part of the supraesophageal lobe makes it the most accessible area for electrode implantation, and it is therefore a good target for testing whether chronic *in vivo* recordings are possible. The cellular anatomy of these lobes is well documented;[9,13] they are found to be a site for adult neurogenesis,[17] and they have been shown to be involved in visual learning.[4] While it is considered a silent area, because electrical excitation of the area does not elicit motor response,[6] recent work in *ex vivo* preparations has shown that robust activity-dependent, long-term potentiation can be induced in this circuit.[11,18,19]

In order to direct and maintain the electrodes in the selected area, we first had to determine the approximate dimensions of the MSF and VL in an adult *O. cyanea*. As there is currently no brain atlas for adult *O. cyanea*, we scanned the brain of a 2.5 kg adult *O. cyanea* and created a 3D volume reconstruction of the tomographic images to estimate the dimensions of the lobes (Figure S1A; see STAR Methods).[20] Based on these measurements, four steel alloy electrodes were cut at 1 and 1.5 mm lengths (see STAR Methods). As octopuses have no skull to which the implanted electrodes can be anchored, but rather a thin cartilage capsule surrounding the central brain, we needed to create a base for the electrodes that can maintain the distance between electrodes and secure their position within the capsule. For this purpose, we cut a semi-rigid plastic card, drilled with 4 holes in line at approximately 1-mm distances. The electrodes were slotted through the card and secured with cyanoacrylate glue (Figure 1E).

## Implantation of logger and electrodes

For surgery, octopuses (n = 3) were removed from the home tank and placed in an anesthetic solution of 2% ethanol in natural seawater (NSW). Logger and electrodes were implanted through a single 2- to 3-cm-long sagittal incision in the skin and muscle layer above the brain capsule, between the eyes (Figures 2A and 2C). Because the tissue is highly elastic, through this

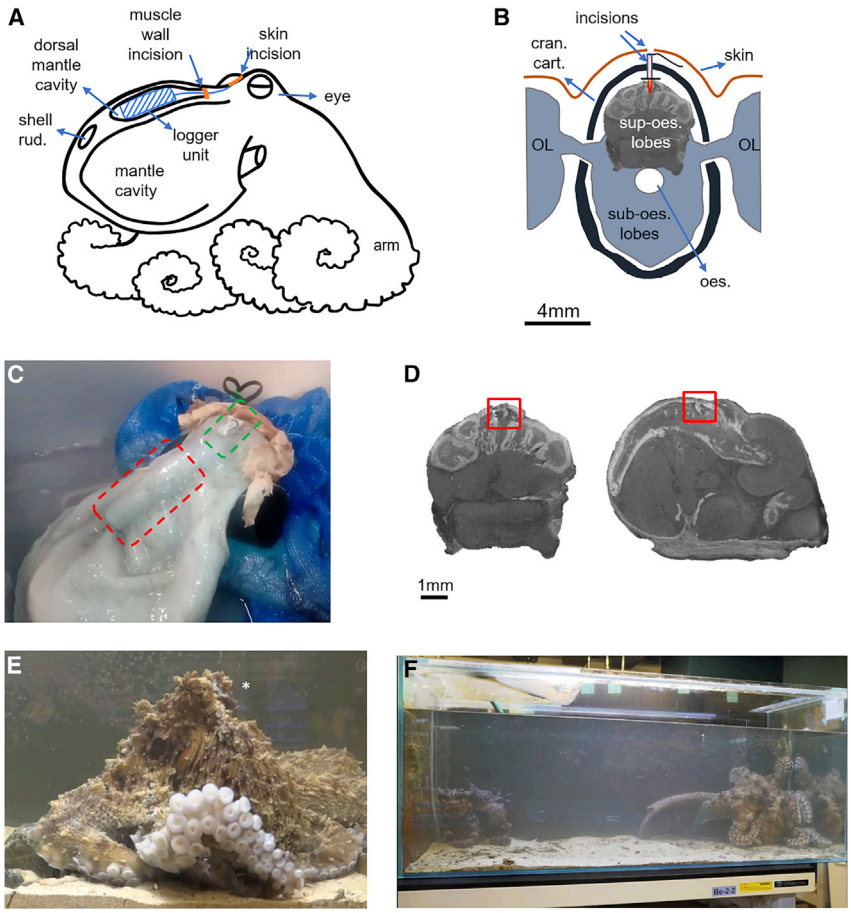


**Figure 2. Surgical method, octopus recovery, and post-experiment electrode location reconstruction**

(A) We made a single incision through the skin above the cranial cartilage, between the eyes. The sealed NeuroLogger unit was inserted into the dorsal mantle cavity through a subcutaneous incision made through the mantle muscle. (Shell rud., shell rudiment).

(B) The brain was exposed with an incision in the cartilage and the electrodes inserted 1–2 mm into the supraesophageal lobes of the brain. The cartilage was closed over the plastic card, securing the electrodes in place. (OL, optic lobe; sup-oes. lobes, supraesophageal lobes; sub-oes. lobes, sub-oesophageal lobes; oes, oesophagus).

(C) Octopus during implantation surgery. The logger unit is secured in the mantle muscle (red dashed box), and the electrode wires are visible prior to closing the incision (green dashed box). The skin is then closed with cyanoacrylate glue over the wires.

(D) Electrolytic burn marks (red boxes) were used to identify electrode location from reconstructed 3D volume rendering of microCT scans.

(E) Following surgery, the octopus was returned to the home tank for recovery. The location of the single incision in the skin is visible as a white line between the eyes (marked by the white asterisk).

(F) Full HD camera view of the awake implanted octopus in the home tank.

incision, we could access the upper mantle muscles and make an incision into the left dorsal mantle cavity. The cavity was expanded using a large stainless steel spatula, and the logger unit was placed in it with connector wires facing out. The incision in the muscle was closed around the wires with cyanoacrylate glue (Figure 2A). We then made a single sagittal incision in the brain capsule, exposing the supraesophageal brain. This incision was held open using scissor clamps, the electrode implant was inserted into the brain, and the reference electrode was placed on the brain surface. The capsule was then closed over the plastic card and secured with cyanoacrylate glue (Figure 2B). Finally, the skin incision was closed and glued, covering all the connecting wires (Figure 2C). The anesthetized octopus was then returned to the home tank for recovery (Figures 2E and 2F).

## Reconstruction of electrode location

At the end of the recording period, octopuses were euthanized in a 4% ethanol NSW solution. The wires connecting the logger unit and electrodes were cut, and the logger unit was removed. Prior to removal of the brain, the location of the electrodes was marked by applying a short electric current to the wires. The dissected brain was then processed for microCT scanning (see STAR Methods). The location of the electrodes was manually determined from reconstructed volumes (Figures 1D, 2D, S1A, and S1B).

## Behavioral data

To collect behavioral data, we filmed the entire duration of the recording with an ultra-sensitive HD camera at 30 frames/s (Figure 2F). Video analysis showed that all three animals rapidly recovered from the anesthesia and regained color and posture within 5 min of being returned to the home tank. Importantly, while there was exploration of the skin incision with the arms (Figures 3A–3C), none of the animals attempted to remove the electrodes or the logger. During the recorded period, which spanned from late afternoon into night, the octopuses were free to move within the home tank. Out of the full duration of the recordings, we selected only clearly visible, non-overlapping behaviors, for which we extracted start and stop times. We annotated periods of general motion, such as general motion of the animal in place, as well as locomotion in which the animals moved around the tank (Figure 3J). Additionally, we found periods of awake immobility and periods identified by behavioral criteria as sleep,[15,21–23] both inside and outside the den (Video S1). As has been shown in several other octopus species, we observed two types of sleep, quiet sleep and active sleep.[21–23] During quiet sleep, the octopus was motionless, the body color was pale, and the pupils were narrow or completely closed (Figures 3C and 3H). Some quiet sleep periods also transitioned into active sleep, in which rapid sucker movement and color/pattern changes were observed (Figures 3A and 3I). Sleep periods were often separated

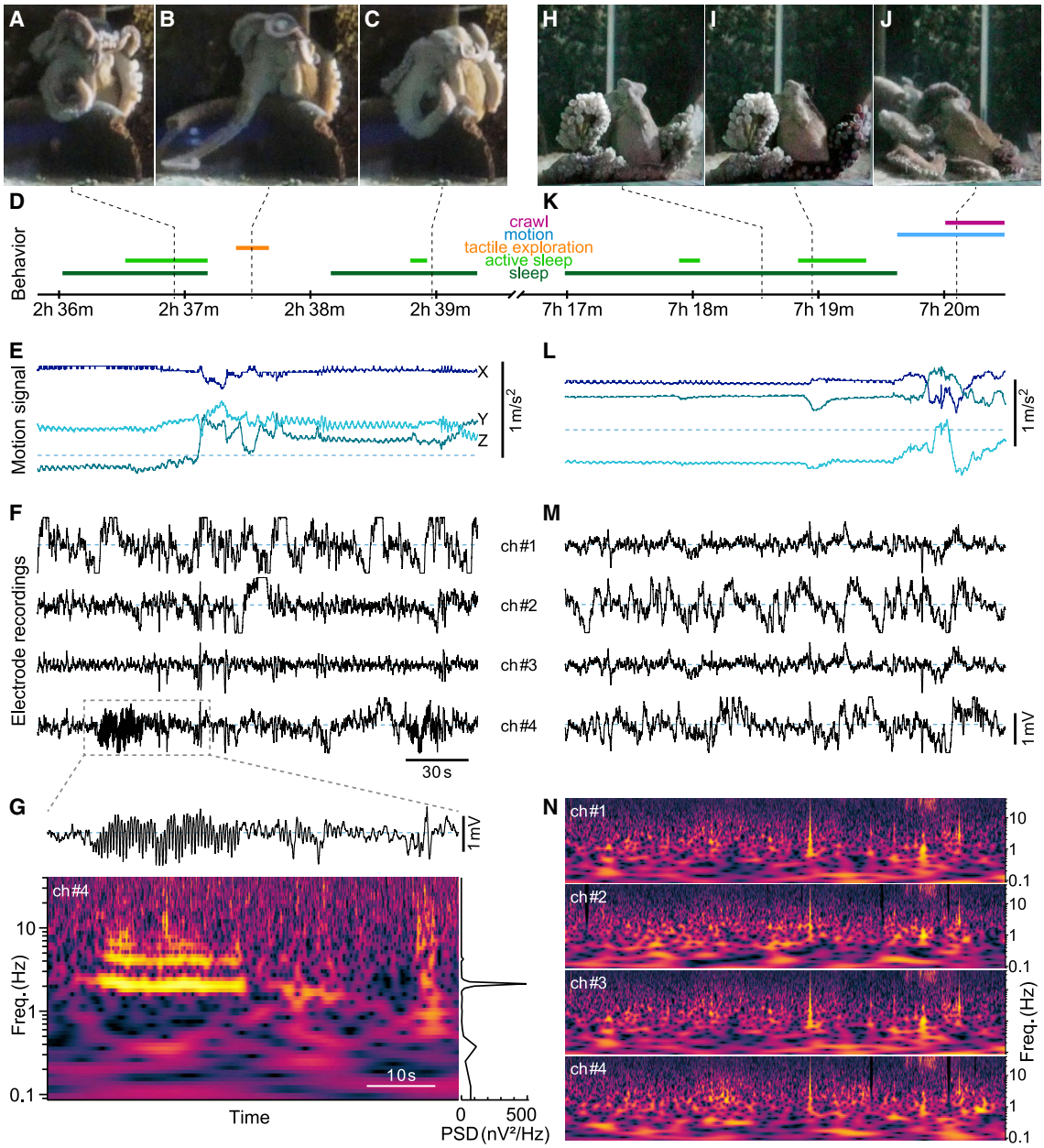


**Figure 3. Merging video and behavioral analysis with recording of motion and brain electrical activity**

Temporal alignment of the data streams from camera and logger (see results), allows us to study the behavioral categorization results, motion signals, and brain activity on the same time axis. Shown here are two 210-s periods that cover a wide range of behaviors and electrical patterns.

(A–C) Three video stills from the first example period (indicated on time axis in D). We observe active sleep (A) with sucker motion and curled and slightly darker arms, tactile exploration (B) with a single arm exploring the substrate, and quiet sleep (C) in a relaxed posture with a general pale color to the entire body.

(D) Shows the intervals with clearly discernible behavior as colored bars above the time axis.

(E) The motion signals complement the behavior analysis, indicating static posture during sleep and increased motion between the sleep episodes. The omnipresent, weak oscillations reflect mantle muscle contractions related to breathing (see also Figure S3 and Video S1).

(F) The electric activity at channels #1 through #4 recorded concurrently with (A)–(E).

(G) Magnification of the 60 s in channel #4 (F; marked by a dashed box), containing a large amplitude, 2 Hz oscillation. Below the trace, the time-frequency analysis of this period is shown. It is obtained with continuous wavelet transformation and the signature of the oscillation stands out. The strong harmonics indicate that the waveform is pointy, in this example with rounder peaks and sharp troughs. For the display, the data is normalized per frequency (see STAR Methods section spectral analysis), and no global color scale can be given.

(H–J) Three video stills from the second 210-s example period, more than 7 h into the approximately 11-h recording (indicated on the time axis in K). While the octopus is at the front of the tank, we observe quiet sleep (H) with a visibly closed pupil and pale body, which transitions into active sleep (I), in which only the chromatophores on the right side of the octopus flash dark. After waking, the animal crawls toward the back of the tank (J).

*(legend continued on next page)*

or followed by cleaning/grooming behavior or tactile exploration of the tank surface by single arms (Figure 3B).

### Data stream fusion

Brain recordings and motion data were recorded by the implanted data logger, while the external camera provided the movies for behavior assessment. We established a common time frame for the two recording devices through a synchronization by IR pulses prior to the implantation. This was confirmed through well-delineated, sudden motions of the animal that were detected on camera and in the logger's accelerometer. This analysis revealed that the camera clock lagged by 0.1 s per recorded hour relative to the logger's clock. For our approximately 12-h recordings, we therefore established a sub-second precise time frame to fuse the data streams.

### Data analysis

For an initial assessment of the data, we displayed behavioral categorization, motion signals, and brain signals on the same time axis (Figures 3A–3F and 3H–3M). Our first observation was the close correspondence between motion signals and animal position changes observed on camera (Figures 3D, 3E, 3K, and 3L). Even breathing motion, which was visually observable in video recordings, was detected by the accelerometer as regular, weak signal undulation (Figures 3E, 3L, and S3A). As these are the first recordings of their kind, from untethered, freely moving cephalopods, prior to a detailed evaluation of the brain signals, we checked for possible signal contamination by motion artifacts or external sources. Visual inspection and correlation analysis showed no evidence of any relation between animal locomotion and brain signals. Amplitudes and spectral composition of the latter show no obvious change when the motion drastically changes between periods of motion and periods of no motion. In a small number of episodes, in which brain signals showed a component very similar to the concurrent breathing rhythm, we found that the phase between the two periodic signals drifted rapidly. We could therefore exclude the contraction of the mantle muscles during breathing as a source of the recorded signals. To check for contamination by external signal sources, we screened for high-frequency signals coincident at all four electrodes. Low-frequency signals would most likely be blocked by the saline-filled tank, and if the high-frequency signals are transmitted, they should impinge on all electrodes. However, when we identified coincident signals, those were still much slower than what we observe as typical external signals that are picked up with metal electrodes (Figures 3M and 3N, just before 7 h 19 min with a half-width of 300 ms). In conclusion, we found that the recorded brain signals were largely free of artifacts from animal motion or external noise sources.

We then obtained a first overview of the temporal and spatial scales on which the data vary by analysis of the spectral content of individual data channels and the cross-correlations between those channels (Figure S1D). The electrical signals are dominated by very low frequencies, and above approximately 1 Hz, the amplitudes fall off very steeply (Figure S1C). We attribute the dominance of low frequencies in part to the large electrode surface, which likely caused some spatial signal averaging and may have contributed to an attenuation of higher-frequency signals.

To examine the spatial scale over which the signals vary, we studied the Pearson correlation coefficient between the electric signals of different electrodes (always excluding the short intervals of signal saturation). We were surprised to find that cross-correlations alternated between almost 1 and −1 on various timescales (Figure S1D) and that neither the electrodes' spatial proximity nor their positioning in the same lobule is a predictor of correlation strength. In all animals, the highest signal correlation occurred between electrodes placed in different lobes or lobules. And in animals 2 and 3, the highest correlation occurred in non-neighboring electrodes, placed 2 mm apart, with weaker correlations to the interjacent electrode. Signals went in and out of synchrony for varying time intervals, and we did not detect a connection between correlation switching and the behavioral state of the animals.

For detailed signal exploration, enabling the identification of patterns from impulses to oscillations, we employed continuous wavelet transformation (CWT) with complex Morlet wavelets. We chose this method over short-time Fourier transform, because CWT allowed us to use different time resolutions for each frequency band. We used time resolutions from 37 s at 0.05 Hz to 125 ms at 40 Hz (Figure 3) and 15 ms at 100 Hz (Figure S2E). In the 2D color maps of the CWT, we identified activity patterns recurring in each of the three animals:

(1) High power oscillations with a basic frequency around 1.5–3 Hz and two to four harmonics (ch#4 in Figures 3F and 3G): these oscillations appeared at times independently on single electrodes (Figures 3F, 3G, and S2A; Video S1) and in other cases, synchronously over several or all four electrodes (Figure S2B). In each animal such oscillations occurred in at least three of the four electrodes, with no clear preference for any lobe or lobule. A connection to behavior was not apparent, although the oscillations often appeared more frequently at certain time periods.
(2) Very slow, large-scale electrical transients (Figure S2C): we consider these a basic constituent of the detected activity, because they can appear on top of an otherwise rather quiet background and are distinct by the succession of a positive and a negative transient over a total duration of 15–45 s. The precise duration as well as the frequency of occurrence vary throughout the recording.

(K–M) As in (D)–(F), behavioral analysis, motion signals, and electrical activity, but for the second 210-s period. In (M), note the striking similarity between the signals from channels #1 and #3. Earlier, the signal correlation was negligible, now it is above 0.9 (see Figure S1D, animal 3 for more detail).
(N) The continuous wavelet transformations for the signals from all four channels in (M), normalized as in (G). A comparison to (M) demonstrates the sensitivity of the method. High-power, transient signals are easily identified by their vertical bright lines. At the same time, slow events and oscillations are equally well detected. For example, the bright signal in channel #4 around 0.8 Hz, starting at 7 h 20 min 15 s, corresponds to 4 transients, appearing at 1.2-s intervals in the channel #4 signal in (M). The regularity and timing of their appearance is immediately evident from the continuous wavelet transformation. Dotted lines in (F), (G), and (M) represent zero signal amplitude. See also Figure S2 and Video S1.

They can occur in combination with other activity patterns. In the time-frequency analysis, these events show as infra-slow waves with frequency components around 0.01 Hz (Figure S2D).

(3) Individual transients with rise times around 10–50 ms and decay time constants of 100–200 ms (Figure S2E): their peak amplitudes vary over more than an order of magnitude and occasionally exceed the 2 mV range of our recording equipment. At different times during the recording, we observed at single recording sites similar transient shapes with opposite signs.

## DISCUSSION

Our study demonstrates that it is possible to record extracellular brain activity from freely moving, untethered *O. cyanea* using implanted data loggers. Although there have been significant advancements in recording brain activity from freely moving fish,[14] these methods could not be adapted to octopuses. The extreme manipulation abilities of octopus arms required us to implant the data logger inside the dorsal mantle cavity. This, and the saltwater environment, blocked remote access to the logger during the recording period, thus restricting the experiment to a single recording session. However, a single experiment can provide over 11 h of electrophysiological and motion data, which can be synchronized with video recordings of behavior, with sub-second accuracy, using preimplantation, external IR signals. Importantly, the general behavior of the implanted animals, which moved around the home tank freely, was not significantly altered by the logger implant, and recorded data was not contaminated by motion artifacts.

Given the size and shape of the waterproofed logger unit, our method is transferable to any large octopus species with sizes similar to the *O. cyanea* studied here.This includes one of the most widely studied species, *Octopus vulgaris*, for which more behavioral, physiological, and genetic knowledge is available.[6,11,15,17–19,22–24]

For our first brain recordings from untethered, freely moving octopus, we targeted the MSF-VL complex, a well-studied and readily accessible area. The octopus's flexible body, together with the lack of tested protocols such as stereotaxic atlases, complicates reproducible electrode insertions. Here, we used measurements from the reconstructed adult octopus brain as guidance and successfully placed all electrodes in the target area. We expect that through similar measurements, deeper brain areas within the supraesophageal lobes can be targeted with adapted electrodes.

The majority of the supraesophageal lobes, among which are the MSF and VL, are reported to be involved in memory formation, consolidation, and decision-making. For example, parts of the frontal lobe system (Figures 1C and S1A), anterior to our recording site, are associated with tactile and chemo-tactile learning. In these areas, tracing studies have also identified a potential reward circuit, which receives sensory inputs from arms and mouth, from which output fibers feedback to sensory organs or up to the VL system.[9,11,25] Other areas, such as the basal lobes in the ventral most part of the supraesophageal brain (Figure S1A), are responsible for the control of complex motor actions.[6,11] These areas would likely have higher activity levels, especially during locomotion, than those recorded in our experiment. Primary sensory input areas and lower motor control areas, which connect to the arms, body, and chromatophores, are found in the suboesophageal lobes. The ability to target these deeper brain areas, without disrupting the animal's behavior, remains to be determined.

Because this is one of the first studies correlating brain activity with behavior in the octopus, we opted to examine the brain signals with a broad scope, using time-frequency analysis to pick up temporal or spectral patterns in a wide range of frequencies and amplitudes. This initial characterization was complicated further because we could not identify any robust correlation between the animals' behavior and the activity in the MSF-VL circuit. Therefore, we only report very distinct activity patterns, which occasionally appeared atop low background activity. One surprising feature of these patterns is their considerable magnitude. We posit that it is associated with the distinct cellular organization of the MSF-VL circuit, which has been likened to the organization of hippocampal circuits.[9,25,26] For example, in vertebrates, such large amplitudes, as we found in the individual transients (Figure S2E), have been observed when sheet-like neuron populations receive concurrent input onto spatially structured input laminae, for example, in CA1 upon stimulation of Schaffer collaterals.[27–29] Like the hippocampus, the MSF-VL network is organized as a matrix of crossing fibers, with large numbers of parallel inputs from the MSF innervating *en passant* millions of tightly packed VL interneurons.[9,11,18] Here, we observed individual transient shapes with opposite signs at a single recording site. These might originate from two different neuronal populations that are both sensed by the same electrode. Alternatively, the signal could stem from a single population that receives, at different times, inputs that differ in sign or origin. Notably, spontaneous signals of very similar time course were observed in developing human-derived neural tissue.[30]

While we could not identify regularities with respect to the subset of general behaviors we observed, this is in line with the known function of the MSF-VL circuit. This system is essential for the consolidation of new memories, yet removal of these areas does not cause substantial deficiencies in general behavior and motion. Therefore, we suggest that by applying this method in combination with targeted repeated behavior, such as visual learning paradigms, the function of the MSF-VL circuit and its role in visual memory and recall can be explored.

This method for recording brain activity from untethered, freely moving octopus can be rapidly adapted by other groups and potentially expanded to other octopus species. Many of the current topics being addressed in cephalopod research today, from learning and cognition to brain states and anesthesia, activity cycles, and social behavior and motor control, can benefit greatly from implementing this method.

## STAR★METHODS

Detailed methods are provided in the online version of this paper and include the following:

- KEY RESOURCES TABLE
- RESOURCE AVAILABILITY

## SUPPLEMENTAL INFORMATION

Supplemental information can be found online at https://doi.org/10.1016/j.cub.2023.02.006.

## ACKNOWLEDGMENTS

We would like to thank OMSS staff for their dedicated support, namely, Koichi Toda, Nobuo Ueda, and Kosuke Mori. Special thanks to Jonathan Miller, Keishu Asada, Teresa Iglesias, Zdeněk Lajbner, and members of the Physics and Biology Unit at OIST. Funding was provided by the Kakenhi C Project code no. 17K07493 (for details please see https://nrid.nii.ac.jp/nrid/1000010790280/) and the Physics and Biology Unit of the Okinawa Institute of Science and Technology Graduate University. Neurologger development was made possible thanks to funding from SNFS3152A0-101706/1 "the neurobiology of pigeon homing—recording flight paths and electrical brain activity" and SNFS3100A0-108446 "approaching the neurobiology of large-scale spatial cognition." A.C. was supported by PSRP-2010-2010 (Polish-Swiss-Research Programme) to H.-P.L.

## AUTHOR CONTRIBUTIONS

Conceptualization, T.G., H.-P.L., and M.J.K.; methodology, T.G., A.C., and M.J.K.; investigation and analysis, T.G., A.N., A.C., F.Z.-K., and M.J.K.; writing—original draft, T.G. and A.N.; writing—review and editing, T.G., A.N., A.C., F.Z.-K., A.D.C., H.-P.L., and M.J.K.

## DECLARATION OF INTERESTS

TSE-Systems has bought all shares of NewBehavior LLC from H.-P.L., who acts occasionally as a consultant for former NewBehavior products.

Received: December 15, 2022
Revised: January 25, 2023
Accepted: February 1, 2023
Published: February 23, 2023

## REFERENCES

1. Darmaillacq, A.-S., Dickel, L., and Mather, J. (2014). Cephalopod cognition. In Cephalopod Cognition, A.-S. Darmaillacq, J. Mather, and L. Dickel, eds. (Cambridge University Press).
2. Hochner, B., and Glanzman, D.L. (2016). Evolution of highly diverse forms of behavior in molluscs. Curr. Biol. *26*, R965–R971. https://doi.org/10.1016/j.cub.2016.08.047.
3. Hanlon, R.T., and Messenger, J.B. (2018). Cephalopod Behaviour, Second Edition (Cambridge University Press). https://doi.org/10.1017/9780511843600.
4. Wells, M.J. (1978). Octopus: Physiology and Behaviour of an Advanced Invertebrate (Springer Netherlands). https://doi.org/10.1007/978-94-017-2468-5.
5. Hochner, B. (2012). An embodied view of octopus neurobiology. Curr. Biol. *22*, R887–R892. https://doi.org/10.1016/j.cub.2012.09.001.
6. Zullo, L., Sumbre, G., Agnisola, C., Flash, T., and Hochner, B. (2009). Nonsomatotopic organization of the higher motor centers in octopus. Curr. Biol. *19*, 1632–1636. https://doi.org/10.1016/j.cub.2009.07.067.
7. Gutnick, T., Byrne, R.A., Hochner, B., and Kuba, M. (2011). Octopus vulgaris uses visual information to determine the location of its arm. Curr. Biol. *21*, 460–462. https://doi.org/10.1016/j.cub.2011.01.052.
8. Gutnick, T., Zullo, L., Hochner, B., and Kuba, M.J. (2020). Use of peripheral sensory information for central nervous control of arm movement by octopus vulgaris. Curr. Biol. *30*, 4322–4327.e3. https://doi.org/10.1016/j.cub.2020.08.037.
9. Young, J.Z. (1971). The Anatomy of the Nervous System of Octopus vulgaris (Clarendon Press).
10. Nixon, M., and Young, J.Z. (2003). The Brains and Lives of Cephalopods (Oxford University Press).
11. Gutnick, T., Shomrat, T., Mather, J., and Kuba, M. (2016). The cephalopod brain: motion control, learning, and cognition. In Physiology of Molluscs, S. Saleuddin, and S. Mukai, eds. (Apple Academic Press), pp. 139–177. https://doi.org/10.1201/9781315207117-5.
12. Chung, W.-S., Kurniawan, N.D., and Marshall, N.J. (2022). Comparative brain structure and visual processing in octopus from different habitats. Curr. Biol. *32*, 97–110.e4. https://doi.org/10.1016/j.cub.2021.10.070.
13. Stern-Mentch, N., Bostwick, G.W., Belenky, M., Moroz, L., and Hochner, B. (2022). Neurotransmission and neuromodulation systems in the learning and memory network of Octopus vulgaris. J. Morphol. *283*, 557–584. https://doi.org/10.1002/jmor.21459.
14. Vinepinsky, E., Donchin, O., and Segev, R. (2017). Wireless electrophysiology of the brain of freely swimming goldfish. J. Neurosci. Methods *278*, 76–86. https://doi.org/10.1016/j.jneumeth.2017.01.001.
15. Brown, E.R., Piscopo, S., De Stefano, R., and Giuditta, A. (2006). Brain and behavioural evidence for rest-activity cycles in Octopus vulgaris. Behav. Brain Res. *172*, 355–359. https://doi.org/10.1016/j.bbr.2006.05.009.
16. Vyssotski, A.L., Serkov, A.N., Itskov, P.M., Dell'Omo, G., Latanov, A.V., Wolfer, D.P., and Lipp, H.-P. (2006). Miniature neurologgers for flying pigeons: multichannel EEG and action and field potentials in combination with GPS recording. J. Neurophysiol. *95*, 1263–1273.
17. Bertapelle, C., Polese, G., and Di Cosmo, A. (2017). Enriched environment increases PCNA and PARP1 levels in octopus vulgaris central nervous system: first evidence of adult neurogenesis in Lophotrochozoa. J. Exp. Zool. B Mol. Dev. Evol. *328*, 347–359. https://doi.org/10.1002/jez.b.22735.
18. Hochner, B., Brown, E.R., Langella, M., Shomrat, T., and Fiorito, G. (2003). A learning and memory area in the octopus brain manifests a vertebrate-like long-term potentiation. J. Neurophysiol. *90*, 3547–3554. https://doi.org/10.1152/jn.00645.2003.
19. Shomrat, T., Zarrella, I., Fiorito, G., and Hochner, B. (2008). The octopus vertical lobe modulates short-term learning rate and uses LTP to acquire long-term memory. Curr. Biol. *18*, 337–342. https://doi.org/10.1016/j.cub.2008.01.056.
20. Metscher, B.D. (2009). MicroCT for developmental biology: A versatile tool for high-contrast 3D imaging at histological resolutions. Dev. Dyn. *238*, 632–640. https://doi.org/10.1002/dvdy.21857.
21. Medeiros, S.L.S., Paiva, M.M.M., Lopes, P.H., Blanco, W., Lima, F.D., Oliveira, J.B.C., Medeiros, I.G., Sequerra, E.B., de Souza, S., Leite, T.S., et al. (2021). Cyclic alternation of quiet and active sleep states in the octopus. iScience *24*, 102223. https://doi.org/10.1016/j.isci.2021.102223.
22. Meisel, D.V., Byrne, R.A., Kuba, M., Mather, J., Ploberger, W., and Reschenhofer, E. (2006). Contrasting activity patterns of two related Octopus species, Octopus Macropus and Octopus vulgaris. J. Comp. Psychol. *120*, 191–197. https://doi.org/10.1037/0735-7036.120.3.191.

23. Meisel, D.V., Byrne, R., Kuba, M., Griebel, U., and Mather, J.A. (2003). Circadian rhythms in Octopus vulgaris. Berl. Paläontol. Abh. *3*, 171–177.

24. Zolotarov, G., Fromm, B., Legnini, I., Ayoub, S., Polese, G., Maselli, V., Chabot, P.J., Vinther, J., Styfhals, R., Seuntjens, E., et al. (2022). MicroRNAs are deeply linked to the emergence of the complex octopus brain. Sci. Adv. *8*, eadd9938. https://doi.org/10.1126/sciadv.add9938.

25. Young, J.Z. (1964). A Model of the Brain (Clarendon Press).

26. Hochner, B., Shomrat, T., and Fiorito, G. (2006). The octopus: A model for a comparative analysis of the evolution of learning and memory mechanisms. Biol. Bull. *210*, 308–317. https://doi.org/10.2307/4134567.

27. Herreras, O. (2016). Local field potentials: myths and misunderstandings. Front. Neural Circuits *10*, 101.

28. Herreras, O. (1990). Propagating dendritic action potential mediates synaptic transmission in CA1 pyramidal cells in situ. J. Neurophysiol. *64*, 1429–1441. https://doi.org/10.1152/jn.1990.64.5.1429.

29. Buzsáki, G. (2002). Theta oscillations in the hippocampus. Neuron *33*, 325–340. https://doi.org/10.1016/S0896-6273(02)00586-X.

30. Trujillo, C.A., Gao, R., Negraes, P.D., Gu, J., Buchanan, J., Preissl, S., Wang, A., Wu, W., Haddad, G.G., Chaim, I.A., et al. (2019). Complex oscillatory waves emerging from cortical organoids model early human brain network development. Cell Stem Cell *25*, 558–569.e7. https://doi.org/10.1016/j.stem.2019.08.002.

31. Friard, O., and Gamba, M. (2016). BORIS: a free, versatile open-source event-logging software for video/audio coding and live observations. Methods Ecol. Evol. *7*, 1325–1330. https://doi.org/10.1111/2041-210X.12584.

32. Ayachit, U. (2015). The ParaView guide: A parallel visualization application (Kitware, Inc.).

33. Asada, K., Nakajima, R., Nishibayashi, T., Ziadi-Künzli, F., Lajbner, Z., Miller, J., Gutnick, T., and Kuba, M.J. (2021). Improving keeping for octopuses by testing different escape-proof designs on tanks for "big blue octopus" (octopus cyanea). Appl. Sci. *11*, 8547. https://doi.org/10.3390/app11188547.

34. Fiorito, G., Affuso, A., Anderson, D.B., Basil, J., Bonnaud, L., Botta, G., Cole, A., D'Angelo, L., De Girolamo, P., Dennison, N., et al. (2014). Cephalopods in neuroscience: regulations, research and the 3Rs. Invert. Neurosci. *14*, 13–36. https://doi.org/10.1007/s10158-013-0165-x.

35. Fiorito, G., Affuso, A., Basil, J., Cole, A., de Girolamo, P., D'Angelo, L., Dickel, L., Gestal, C., Grasso, F., Kuba, M., et al. (2015). Guidelines for the Care and Welfare of Cephalopods in Research –A consensus based on an initiative by CephRes, FELASA and the Boyd Group. Lab. Anim. *49*, 1–90. https://doi.org/10.1177/0023677215580006.

36. Bakeman, R., and Gottman, J.M. (1997). Observing Interaction: an Introduction to Sequential Analysis, Second Edition (Cambridge University Press). https://doi.org/10.1017/CBO9780511527685.

## STAR★METHODS

### KEY RESOURCES TABLE

| REAGENT or RESOURCE | SOURCE | IDENTIFIER |
|---|---|---|
| Experimental models: Organisms/strains | | |
| *Octopus cyanea* | local fishermen | wild type |
| Software and algorithms | | |
| Amira 6.5.0 | Thermo Fisher Scientific, Waltham, Massachusetts, USA | http://www.thermofisher.com/amira-avizo; RRID:SCR_007353 |
| BORIS | Friard and Gamba[31] | http://www.boris.unito.it/ |
| Igor Pro 9.0.2.1 | Wavemetrics Inc., Portland, OR, USA RRID:SCR_000325 | RRID:SCR_000325 |
| Final Cut Pro 10.6.2 | Apple inc. | N/A |
| Adobe Illustrator | Adobe Inc., 2019 | https://adobe.com/products/illustrator; RRID:SCR_010279 |
| ParaView 5.8.1 | Ayachit[32] | https://www.paraview.org/; http://www.kitware.com/; RRID:SCR_002516 |
| Other | | |
| Neuologger | Newbehavior AG, Zurich, Switzerland | Currently available from: TSE-Systems International, Germany |
| Nickel-metal Hydride Rechargeable batteries | Power One ACCU Plus p312 | N/A |
| ZEISS Xradia 510 Versa 3D X-ray Microscope | Zeiss | https://www.zeiss.co.jp/microscopy/products/x-ray-microscopy/zeiss-xradia-510-versa.html |
| SONY SNC-VB770 | Sony | Discontinued https://www.sony.jp/snc/products/SNC-VB770/ |
| FE 50mm F1.2 GM lens | Sony | SEL50F12GM |
| Blackmagic Video Assist1080HD 7" | Blackmagicdesign | https://www.blackmagicdesign.com/products/blackmagicvideoassist |

### RESOURCE AVAILABILITY

#### Lead contact

Further information and requests for resources should be directed to and will be fulfilled by the Lead Contact, Tamar Gutnick (tamar.gutnick@mail.huji.ac.il).

#### Materials availability

This study did not generate new unique reagents.

#### Data and code availability

- All data reported in this paper will be shared by the lead contact upon request.
- This paper does not report original code.
- Any additional information required to reanalyze the data reported in this paper is available from the lead contact upon request.

### EXPERIMENTAL MODEL AND SUBJECT DETAILS

Adult *Octopus cyanea* (2.5-4.2 kg) were collected by local fishermen on the Okinawan coast of the East China sea. They were individually housed in tanks enriched with live rocks, sand substrate and ceramic pot dens.[33] Octopuses were fed with live/dead crustaceans or dead fish. All tanks were part of a flow-through natural sea water (NSW) system with natural lighting.

All experiments were approved by the OIST animal research committee and adhered to EU Directive 63/2010/EU.[34,35] All experiments were conducted according to - Application for Ethical Approval for Use of Animals (Protocol number: 2017-176) as follows, based on Paragraph 7, Article 13 of the Animal Experiment Regulations at Okinawa Institute of Science and Technology Graduate University.

## METHOD DETAILS

### Data loggers

We used the commercially available data loggers NeuroLogger© (Newbehavior AG, Zurich, Switzerland, now marketed by TSE-Systems International, Germany), originally developed for EEG recording in flying birds and untethered small mammals[16] (Figure 1B).

The NeuroLogger contains 4 input channels for electric signals, 2 reference channels, 3 accelerometer channels and an infrared receiver channel. It features a 1,000 fold signal amplification and a nominal frequency range of 0.5-500 Hz.

In order to record from untethered, freely moving octopuses, the data logger was enclosed in a 6x2 cm airtight waterproof casing. The data logger was powered by 2 Nickel-metal Hydride Rechargeable batteries (Power One ACCU Plus p312) which are voltage compatible with zinc air batteries, but do not require air.

All recorded data is stored on the data logger, and does not require connection to an external computer during the recording. At our sampling frequency of 512 Hz for electric signal and 102Hz for motion signals, we recorded for approximately 12 hours, limited by battery life. After the removal of the logger, the data was downloaded to the computer using dedicated software in hex-file format and converted to.edf files.

### Fabrication of waterproof casing

We created single use, waterproof casings from 2.5 cm diameter heat shrink tubing. To seal the end of the tube we created two end plugs by layering increasing diameters of heat shrink tubing (0.1-2.5 cm diameter, of approx. 1 cm length). One of the plugs included the electrode connector. The blank plug was sealed to the casing tube with low heat and cyanoacrylate glue. At the beginning of the experiment, the data logger was turned on by adding the batteries, synchronized with the video recording by series of external IR flashes, and then placed into the casing tube. The electrode connector end plug was sealed with low heat at the plug location and additional cyanoacrylate glue.

### Fabrication of connector and electrodes

We created the electrode connector end plug by layering increasing diameters of heat shrink tubing (0.1-2.5 cm diameter, length 1 cm) over 5 insulated copper wires. On one side of the plug, the wires were trimmed to 1 cm length and soldered to connector pins. On the other side, the wires were trimmed to 5 cm and the electrodes attached. Steel alloy EEG electrodes (0.2mm diameter) were cut to 1mm (3 electrodes - targeting the VL) and 1.5 mm length (1 electrode - targeting the MSF). These lengths were selected based on measurement from a previously scanned *O. cyanea* brain (Figure 2D; see STAR Methods section X-ray microtomography (micro-CT)). Based on these measurements we cut a 2x6 mm plastic card and drilled 4 holes in a line at 1 mm distances. The electrodes were threaded through the holes insulated with parafilm and secured with cyanoacrylate glue. The reference electrode was separately connected to the remaining wire.

### Surgery

Prior to surgery, we removed the octopus from the home aquarium in a mesh bag and placed it in an opaque container with an anesthetic solution of 2% ethanol in natural seawater (NSW). When the octopus was anesthetized we moved it with the mesh bag to the operating container and exposed only the mantle and head, leaving the arms within the bag. The eyes were covered with NSW soaked tissue. During surgery the gills were irrigated manually with NSW and anesthetic solution.

A 2-3 cm long sagittal incision in the skin and thin muscle layer was made above the brain capsule, starting between the eyes and toward the mantle. Once the skin and muscle were pulled back, an incision was made through the upper mantle muscles into the left dorsal mantle cavity. The incision leading to the pocket was widened using a large stainless-steel spatula (210 mm).

The running NeuroLogger unit, in its waterproof casing, was inserted into the dorsal mantle cavity, with the wires and electrode card remaining outside. When it was in position the incision in the mantle muscle was closed with cyanoacrylate glue, securing the data logger in place.

A small sagittal incision was made through the cartilaginous brain capsule. The sides were clamped open revealing the supraesophageal brain. Small amounts of brain jelly were removed with forceps to allow easier access to the brain.

The electrodes were inserted into the MSF and VL and the reference electrode was placed at the surface of the brain within the brain capsule. The cartilage was then released from the clamps to close above the plastic card. The area was dried and sealed with cyanoacrylate glue. Finally, the skin incision was closed above the wires and sealed with cyanoacrylate glue.

After surgery, the anesthetized, implanted, octopus was returned to the home tank for recovery.

### X-ray microtomography (micro-CT)

Dissected brains were preserved in 4% formaldehyde solution and later transferred to 70% ethanol and dehydrated serially in 80%, 90%, and 100% ethanol. Prior to scanning, each tissue sample was stained with 1% elemental iodine in absolute ethanol

(I2E) for 1-2 days.[20] After staining, samples were washed in absolute ethanol three times. Samples were mounted in 50 ml centrifuge tubes and scanned using a laboratory ZEISS Xradia 510 Versa 3D X-ray Microscope. Samples were wrapped in Kim wipe and soaked in ethanol to prevent moving of the sample within the container and to keep the tissue moist. Tomographic images were acquired using 0.39x objective magnification with source voltages of 80-100 kV, power of 7-9 W, and exposure times of 1-2 s. No beam filter was used.

A combination of voltage, power and exposure time was chosen to yield intensity levels >15,000 across the whole sample. Full 360 degree rotations were done with 1601 projections. Depending on the field of view, the brain samples were imaged at spatial resolution between 8.15 - 27.13 μm/voxel. Scanning duration for each sample was less than 2 h.

Tomographic sections were reconstructed using the integrated volume reconstruction software (XMReconstructor) of the Xradia machine, saved in DICOM file format, and later accessed with Amira software (version 6.5, Thermo Fisher Scientific, Waltham, Massachusetts, USA) for volume rendering and manual segmentation. A gray-scale color map with adjusted opacities for volume renderings and ortho-slices was used to represent the attachment site of the electrode on the brain and to estimate the depth of penetration of the electrode into the MSF and VL (Figures 1D, 2D, and S2A). For brain lobes of the central nervous system (CNS), we segmented the inner, lobular neuropil without its confluent outer perikaryal layer.

The surface generation algorithm implemented in Amira (*Generate Surface* module) was applied for each segmented material using smoothing function values < 2.5. The resulting 3D surface meshes were exported in.ply format and imported into ParaView package for data visualization.[32] Figures for brain lobes were created with Adobe Illustrator (Adobe Inc., 2019; Figure S1A).

### Filming

The experiment was filmed using ultra high-sensitivity SONY SNC-VB770 camera (ISO 100–102400), connected to a 7" BlackMagic Video Assist portable recorder (Blackmagic Design Pty. Ltd.) in 1080 HD resolution at 30 frames per second. The camera was set to automatically adjust to natural light conditions, with filming beginning in daylight and continuing through the night.

The video files were then converted to mp4 format at HD resolution for further analysis.

Video recording and behavioral analysis were synchronized by a series of IR flashes recorded on the NeuroLogger IR channel and visually observable on the video through IR sensitive camera.

### Reconstruction of electrode location

At the end of the experiment octopuses were euthanized in a solution of 4% ethanol in NSW. Prior to the removal of the brain, the location of the electrodes was marked using electrolytic lesions. The supraesophageal brain was then preserved in 4% formaldehyde solution and processed for scanning.

A gray-scale colormap with adjusted opacities for volume renderings and ortho-slices was used to manually estimate the location and the depth of penetration of the electrodes into the MSF and VL (Figure 2D).

## QUANTIFICATION AND STATISTICAL ANALYSIS

### Behavioral analysis

Videos were manually analyzed in BORIS software,[31] by observer agreement of two experienced experimenters.[36]

Start and stop times were recorded only for clearly definable non-overlapping behaviors.

General motion: small movements such as repositioning in place. The mantle contractions associated with breathing were not recorded as motion, and these are observable also in periods in which no other motion is seen.

Locomotion: Crawling, in which the animal maintains contact with the floor of the tank (Figure 3J); Swimming, in which the animal uses the siphon to expel water and propel itself forward with no contact to the surface of the tank.

Sleep: Quiet sleep, in which the octopus was motionless, the body color was pale and the pupils were narrow or completely closed (Figures 3C and 3H); Active sleep, a transition from quiet sleep, in which rapid sucker movement, motion of darkly colored arm tips, and color/pattern changes were observed (Figures 3A and 3I).

Cleaning/Grooming: Coordinated curling of arms over the surface of the body and into the mantle cavity.

Tactile exploration: The octopus sits in a single position and has a single arm exploring the surface of the tank.

To compare breathing rate with recorded motion signals, a 20 minute period in which the octopus was not moving was analyzed. Each breath was marked as a single time point in which the mantle opening closed, just before water expulsion from the mantle (Figure S3C).

### Data stream fusion

Timing: through initial synchronization, and comparison with isolated motion events throughout the recording. We established high accuracy of synchronization between camera and logger, with only 0.1 s /h delay in the camera stream.

### Spectral analysis

For initial assessment, the power spectral density of the electric signals was calculated in Igor Pro 9 (wavemetrics inc.), normalization for sampling rate and duration is applied to obtain a quantitative result. The average power spectral density for one electrode and one animal is calculated for the entire 11.5-12.7 hours of an experiment, starting 15 min after the animal has been returned to the water

and ending several hours later with the end of the experiment. Because of this extensive duration, the power spectral density curves displayed in Figure S1C cover more than 5 orders of magnitude and have been smoothed with narrow Gaussian windows. The window width increased from $f/(20\pi)$ for $f<0.1$ Hz to $f/(4\pi)$ for $f>5$ Hz.

For visualization and pattern detection, the time-frequency-analysis was used. It reports the signal amplitude for various frequency bands in a time-resolved manner. We utilized the continuous wavelet transformation with complex Morlet wavelets, implemented in Igor Pro 9. The shape of the wavelets is described by $\pi^{-1/4} \cdot e^{2\pi i t/T} \cdot e^{-2t^2\pi^2/(T\cdot m)^2}$, where T is the inverse of the wavelet's frequency and m is a free positive parameter, describing the relation between the period T and the width of the Gaussian envelope of the wavelet. This specific transformation can be understood in terms of a simple Fourier analysis: The result of the continuous Morlet wavelet transformation for a frequency $f$ at a time point $t$ is mathematically equivalent to the Fourier component at frequency $f$ obtained from the data multiplied with a Gauss-window centered on time $t$. The temporal resolution of the transformation is approximately equal to the full-width at half-maximum $w_{1/2}$ of this Gauss-window, while frequency resolution is inversely proportional to this width. For frequencies $f<0.05$Hz, this width $w_{1/2}$ was chosen to be $w_{1/2} = \sqrt{2\cdot \ln 2}\cdot m/\pi \cdot T$, with m=5 corresponding to 1.9 periods. As $f$ increases, the parameter m was increased to reach 13 for $f>20$ Hz, corresponding to $w_{1/2}=5$ T. All continuous wavelet transformations shown here were performed with identical $w_{1/2}$ settings. Because $w_{1/2}$ influences not only the frequency resolution, but also the absolute frequency position, the entire time frequency analysis was calibrated with signals composed of pure sinusoids. In all graphs, the frequency axes reflect the correct position of the signal components. To cover the large range of frequencies, typically 0.09 Hz to 40 Hz, the wavelet transformation was calculated at exponentially spaced frequency values and displayed on a log scale.

To make the visualization of the continuous wavelet transformation maximally informative, some form of amplitude normalization across frequencies has to be applied. Otherwise, only the signal components at low frequencies, e.g. 0.01 Hz can be appreciated in the graphs, because the temporal variations in their power is orders of magnitude larger than the variations at high frequencies, such as 20 Hz.

This can be discerned in Figure S2D, where no normalization was applied, specifically to highlight the low-frequency components. There, the color scale corresponds to absolute signal amplitude, as given in the color-scale labels. In all other CWTs, we normalized each frequency component by the average power at this frequency over the analyzed interval. Consequently, the color scale of normalized CWTs reflects power not on an absolute scale, but in units relative to each frequency band's signal average. To heighten contrast for weak changes, we further compressed the data by applying the logarithm. This corresponds to a decibel scale. The normalization of a continuous wavelet transformation for a time interval $\Delta t$ thus reads:

$$CWT_{dB}^{norm}(f,t) = \log(CWT(f,t) / \langle CWT(f)\rangle_{\Delta t}).$$